Inverse Method for Estimating Shear Stress in Machining

T. J. Burns[a,1,*], S. P. Mates[a,2], R. L. Rhorer[a,3], E. P. Whitenton[a,3], D. Basak[b]

[a]National Institute of Standards and Technology, 100 Bureau Dr., Gaithersburg, MD 20899, USA
[b]Orbital Sciences Corp., 21389 Atlantic Blvd., Dulles, Virginia 20166, USA

Abstract

An inverse method is presented for estimating shear stress in the work material in the region of chip-tool contact along the rake face of the tool during orthogonal machining. The method is motivated by a model of heat generation in the chip, which is based on a two-zone contact model for friction along the rake face, and an estimate of the steady-state flow of heat into the cutting tool. Given an experimentally determined discrete set of steady-state temperature measurements along the rake face of the tool, it is shown how to estimate the corresponding shear stress distribution on the rake face, even when no friction model is specified.

Keywords: metal cutting, friction, numerical and analytical modeling, Abel integral equation, AISI 1045 Steel

[*]Corresponding author
Email address: timothy.burns@nist.gov (T. J. Burns)
[1]Information Technology Laboratory
[2]Material Measurement Laboratory
[3]Engineering Laboratory

1. Introduction

After more than three quarters of a century of research in the mechanics of machining processes, a period starting in the early 1890's with the tool-life studies of Taylor (1907) (see, e.g., Kalpakjian and Schmid (2009)), which Usui and Shirakashi (1982) refer to as "descriptive," the introduction of software based on finite element analysis (FEA) methods, beginning in the 1970's (Zienkiewicz, 1971; Kakino, 1971; Shirakashi and Usui, 1976) encouraged the hope that a "predictive" machining theory could be developed, so that important process variables such as spindle speeds, cutting forces, chip thicknesses, and especially peak tool temperatures, could be estimated accurately, and machining operations could be optimized, without requiring expensive trial and error experimentation. However, after almost another half-century of research, and despite the many advances that modern finite-element analysis software packages incorporate, it has become apparent that these models need adjustment and tuning for a given application, and truly predictive software is not yet available.

A major reason for the lack of predictive capability of finite-element based machining models is the lack of good constitutive response models for work materials. It is difficult to estimate the flow stress under extreme conditions of rapid, very large, and localized shearing deformation, heating rates as high as one million degrees C per second, resulting in enormous temperature gradients, and peak temperatures on the order of 1000 °C, in the thin primary shear zone where cutting takes place, and in the secondary shear zone, a thin boundary layer in which the work material continues to deform as it moves along the cutting edge of the tool; see Figure 1. The thickness of this layer decreases with increasing cutting speed (see, e.g., Trent and Wright (2000)), which makes estimates of local variables such as strain extremely difficult to obtain experimentally.

In what follows, we will first review some NIST work on the medium carbon steel AISI 1045. AISI 1045 is widely used in automotive and heavy equipment manufacturing for component parts, such as crankshafts, gears, axles, and connecting rods, because of its machinability, strength properties, and resistance to wear. These are among the reasons that it was the material chosen for the "Assessment of Machining Models" (AMM) study (Ivester et al., 2000), that was performed jointly by the National Institute of Standards and Technology (NIST) and the International Academy for Production Engineering - College International pour la Recherche en Productique (CIRP).

In work performed at NIST that was related to the AMM, new non-

contact thermometric techniques were developed, to image one of the side faces of the tool and of the workpiece, in order to obtain an estimate of the 1D temperature distribution on the tool-chip interface during plane strain, steady-state orthogonal machining tests on AISI 1045 (Davies et al., 2003b). As follow-ons to this study, computer simulations were performed, in an attempt to model the temperature field in the chip. It was found that finite-element simulations, using the commercial software package Abaqus (2003), with a Coulomb sliding friction model to simulate the tool-chip interaction on the rake face, and three different constitutive models for AISI 1045, two of which had been specifically developed for machining simulations, underpredicted the measured peak tool-chip interface temperatures by as much as 300 °C (Davies et al., 2003a). These results, which support the hypothesis that there is too much thermal softening in the constitutive response models for AISI 1045, will be reviewed briefly in Section 2.

Another project related to the AMM work has been the development of the NIST Pulse-Heated Kolsky Bar Laboratory (Mates et al., 2008, 2009). This laboratory combines a split-Hopkinson pressure bar (Rhorer et al., 2002) with a rapid heating and thermal measurement system (Basak et al., 2003; Yoon et al., 2003; Basak et al., 2004; Whitenton, 2005), so that a test sample can be pre-heated in-situ to a specified temperature in a few seconds, prior to loading the sample in compression. Using this laboratory, we have demonstrated that AISI 1045 steel has a significantly stiffer constitutive response when it is rapidly pre-heated, than when it is pre-heated more slowly, on a time scale on the order of minutes (Burns et al., 2012). We will also show in Section 2, that when this stiffer constitutive response is incorporated into a Johnson-Cook constitutive model and used in Abaqus, with the same Coulomb friction model, to simulate the temperature in the chip during orthogonal cutting of AISI 1045, it gives improved peak rake face temperature predictions, but the results still underpredict the temperature by as much as 150 °C.

One area of machining research in which significant progress has been made in the past few years has been the measurement of the 2D temperature distribution on the chip-tool interface, using infrared thermography. In particular, Menon and Madhavan (2015) have reported high accuracy temperature measurements in Ti-6Al-4V, using single wavelength thermography with an instrumented, transparent yttrium aluminium garnet (YAG) tool. For their experimental cutting conditions, which produced shear-localized chips, and measured peak temperatures of 900 °C − 1000 °C, they have obtained a 1D temperature distribution as a function of distance along the rake face of the tool, along an internal cross section of the chip-tool interface, with

an estimated uncertainty in the temperature of less than 6 °C. Motivated by this work, the main purpose of the present paper is to investigate and to provide an affirmative answer to the following theoretical question. Assume that it is possible to obtain good in-situ temperature measurements along an internal 1D cross section of the chip-tool interface during a steady-state orthogonal machining operation, that produces continuous chips. Can these data be used to obtain an estimate of the associated 1D shear stress distribution in the chip near the rake face?

Our approach to addressing this question builds on early theoretical modeling of the chip temperature that was done by Rapier (1954) and Weiner (1955). Rapier assumed that the chip material leaves the primary shear zone, treated as a surface of zero thickness, at a constant temperature, and that the material is further heated by friction as it moves at the cutting speed over the contact region on the tool face. Heat generated by friction was modeled as a boundary condition for a two-dimensional convection-diffusion problem for the temperature field in the chip. By assuming that, in the direction of chip flow, diffusion of heat is negligible compared to convection of heat by mass transport, Rapier was able to reduce the problem to a 1D heat equation, for a strip of chip material in the direction normal to the tool. The heat flux into the chip due to friction, in the direction normal to the rake face, was assumed to be uniform over a contact length that was taken to be proportional to the chip thickness. Weiner made the same reduction to a heat equation in modeling the temperature distribution in the chip produced by uniform heat production in a primary shear zone of zero thickness.

Wright and Trent (1974); Trent and Wright (2000) demonstrated that, in machining at sufficiently high speeds, there is a region of sticking, or seizure, on the rake face in the material that emerges from the primary shear zone, up to some distance L_p from the tooltip along the rake face. In a thin layer within the chip along this region, there is a "flow zone" in the chip, in which the bottom of the zone is bonded to the tool, while the top of this zone moves with the speed of the bulk of the chip. In this region, Wright and Trent assumed a constant rate of heat generation per unit area. For the remainder of the length of contact $L_c - L_p$ along the rake face, Wright and Trent argued, citing the work of Zorev (1963), that sliding takes place, and the rate of heat production decreases linearly to zero, where the chip loses contact with the tool. Subsequently, using Rapier's model with this assumed variable heat source on the rake face, Wright et al. (1980) showed that predicted temperatures were in very good agreement with experimentally measured temperatures in cutting experiments on pure

copper. An important feature of this analysis is that it takes into account that a significant percentage of the heat generated by friction is absorbed by the tool. In the past few years, some related nonlinear "two-zone" tool-chip rake face friction models have been developed by Ozlu et al. (2009, 2010).

Our modeling approach is also related to that of Moufki et al. (1998), who estimated the temperature on the tool-chip interface, with the assumption that the friction depends on the mean temperature in the chip along its surface of contact on the rake face. Like Rapier and Weiner, Moufki et al. neglected the secondary shear zone, and assumed that convection dominates diffusion in the direction of chip flow. Heat production in the primary shear zone was modeled using a method that had been developed by Dudzinski and Molinari (1997), which treated this region one-dimensionally, as a thin stationary shear band of uniform thickness, in which the thermoviscoplastic properties of the deforming chip material were used to determine its temperature on exiting the cutting region. Heat production by friction on the rake face was taken into account by a boundary condition, in which the heat flux into the material in the direction normal to the rake face was directly proportional to the pressure, the cutting speed, and the mean coefficient of friction. The problem was solved iteratively in the temperature to determine the friction coefficient.

More recently, Molinari et al. (2011, 2012), using analytical and numerical modeling methods, performed a detailed study of the material response behavior in orthogonal cutting of a mild steel in the region near the tool-material contact along the rake face. They used a friction law due to Zorev (1963), which specifies that when sliding occurs, $\tau = \mu\sigma$, where τ is the shear stress on the rake face, σ is the normal stress, and μ is a parameter (assumed to be constant) that is a characteristic of the interface; when sticking occurs, $\tau < \mu\sigma$, and in fact, the shear stress τ in the chip is related to the von Mises equivalent flow stress σ_{eq} by $\tau = \sigma_{eq}/\sqrt{3}$, so that the shear stress in the material and the shear flow stress are equal, $\tau = \tau_y$. Thus, if the shear stress in the work material on the tool-work interface could be determined when there is a sticking region, this would provide useful constitutive response information. Furthermore, Molinari et al. (2012) demonstrated that there is necessarily a thin secondary shear zone that is set up when sticking occurs, with a thickness that decreases to what appears to be an asymptotic value with increasing cutting speed. Inside this thin layer, the chip material deforms in simple shear, as its velocity increases from zero to the velocity of the bulk of the chip, which moves as a rigid body in the direction parallel to the rake face.

Instead of trying to estimate the temperature distribution in the chip and

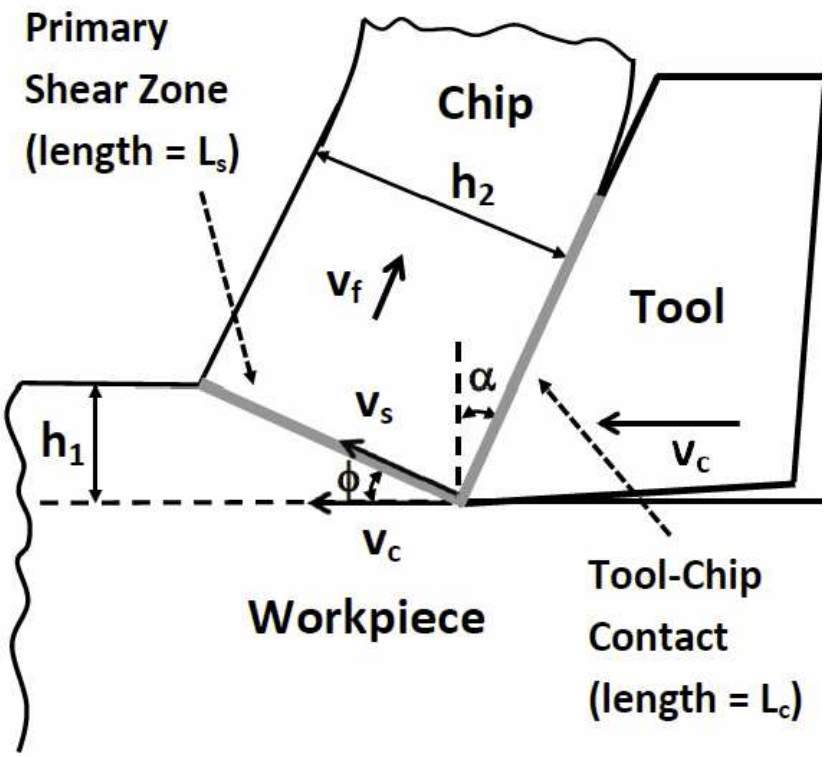

Figure 1: Idealized model of chip flow in orthogonal cutting.

the tool, given a model for the flow stress in the work material, our goal here is to obtain an estimate of the shear stress in the chip in a thin layer near the rake face. Our approach is based on a detailed analysis of heat generation in the chip, using a two-zone contact model, that also neglects the secondary shear zone. This model was developed by Tlusty, and is presented in detail in Tlusty (2000). The model, which we will refer to as Tlusty's Method, was used by Davies et al. (2003b), as an independent means of verifying that their experimental temperature measurements during orthogonal cutting of AISI 1045 steel were plausible. Tlusty's Method will be summarized in Section 3. Since it is based on empirical data from machining experiments, as well as on simplified models of heat production and heat transfer into the tool along the rake face, and somewhat arbitrary assumptions about the lengths of the sticking and sliding regions, it follows that this method is also in the category of "descriptive," and not "predictive," machining models. Nevertheless, the model has the virtue of being simple enough to analyze in detail. Using singular perturbation theory, we will show in Section 4 that an analysis of this model, and in particular of how it estimates the friction power on the tool-chip interface, taking into account the steady-state flow of heat into the tool, suggests an inverse method for estimating the shear stress in the work material on the rake face.

In Section 5, we will show that the analytical approach in Section 4 can be generalized. An inverse method will be presented, that is based on deconvolution and unfolding of a Volterra integral equation of the first kind (cf. Wing (1991)), such that, given an experimentally determined discrete set of steady-state temperature measurements along the rake face of the tool, the stress distribution in the chip material on the tool-chip interface can be estimated, even when no interface friction model is specified. While we would prefer to demonstrate our method using the temperature data in Menon and Madhavan (2015), the titanium alloy chips in these experiments were shear localized. Therefore, we will present instead an application of this model to the temperature data from cutting experiments on AISI 1045 steel, that are discussed in Davies et al. (2003b).

We will conclude with a brief discussion of the inadequacy of constitutive models such as the Johnson-Cook model for machining simulations, and some final remarks, in Section 6.

2. Review of Experimental and Computational Temperature Results

For modeling purposes, the simplest, and most fundamental, machining operation is orthogonal cutting, in which the deformation process can be treated as one of plane strain; see, e.g., Merchant (1944); Shaw (1984); Oxley (1989). In the thin primary shear zone where cutting takes place, it is not uncommon, in alloys of interest in manufacturing, to have shear strains on the order of $\epsilon = 2$, shear strain rates on the order of $\dot{\epsilon} = 10^4\,\mathrm{s}^{-1}$, and heating so rapid that the local workpiece temperature increases from ambient to greater than 50 % of the melting temperature, in a time on the order of tens of microseconds. Along the secondary shear zone, in the contact region between the tool face and the chip material (see Figure 1), there is typically both sticking and sliding friction. This friction causes additional rapid shearing and very large deformation of the chip material in a thin boundary layer along the tool-chip interface, which leads to additional heat generation in both the work material and the tool, on a time scale on the order of a hundred milliseconds. As discussed in the Introduction, our focus in this paper is mainly on the region in the chip near the tool-chip interface.

In a series of steady-state orthogonal dry cutting experiments with a carbide tool on AISI 1045 steel, non-contact thermometric methods were used to determine the steady-state temperature field in the chip, with a resolution of $5\,\mu$m, under conditions of continuous chip formation (Davies et al., 2003b). In four sets of these experiments, the tool rake angle was $\alpha = 0$, the cutting speed and the chip width were kept fixed, with $v_c = 3.7\,\mathrm{m/s}$ and $b = 1.5\,\mathrm{mm}$, respectively, but the uncut chip thickness h_1 was changed for each set; see Table 1.

Case	h_1 (μm)	h_2 (μm)	r	ϕ (deg)	v_f (m/s)
1	48	160	.300	16.7	1.10
2	40	145	.276	15.4	1.01
3	31	125	.248	13.9	.932
4	23	100	.230	13.0	.866

Table 1: Data from four sets of orthogonal cutting experiments; h_1 and h_2 are the uncut and cut chip thicknesses, respectively; r is the chip thickness ratio; $\phi = \tan^{-1} r$ is the shear plane angle; and $v_f = r\,v_c$ is the chip velocity.

In a follow-on to these experiments (Davies et al., 2003a), the finite-element analysis package Abaqus (2003) was employed to model the four orthogonal cutting tests. CPE4RT elements were used, and chip separation

was controlled by a failure model based on a critical value of the effective plastic strain. The sharp, 0° rake angle, cemented tungsten carbide tool insert that was used in the experiments was modeled as an elastic, heat-conducting wedge, with zero edge radius. Its response was essentially rigid due the large elastic modulus of the carbide relative to that of the workpiece material. A standard Coulomb friction model, with constant coefficient of friction μ, was used to simulate the interaction of the tool and workpiece material along the rake face, with the shear stress τ given by

$$\tau = \min(\tau_y, \mu\sigma). \tag{2.1}$$

Here, $\tau_y = \sigma_{eq}/\sqrt{3}$, where $\sigma_{eq}(\epsilon, \dot{\epsilon}, T)$ is the local value of the von Mises flow stress of the AISI 1045, ϵ and $\dot{\epsilon}$ are the effective plastic strain and strain rate, and T is the local temperature; σ is the local value of the normal stress. The coefficient of friction was assigned the value $\mu = 0.27$, based on a literature search (Davies et al., 2003a).

Three different empirical constitutive response models were considered for the flow stress of the AISI 1045 workpiece material in the computer simulations reported in Davies et al. (2003a). The first two models were due to Jaspers and Dautzenberg (2002): a Johnson-Cook model (Johnson and Cook, 1983), and a Zerilli-Armstrong model (Zerilli and Armstrong, 1987), both of which had been determined specifically for use in machining simulations of AISI 1045. The thesis work of Jaspers (1999) included a systematic effort to identify the levels of strain, strain rate, and temperature in AISI 1045 (and two additional alloys) during a high-speed metal cutting operation on this material. Testing methods, including a split-Hopkinson pressure bar facility (SHPB) with a system for pre-heating a material sample prior to loading it in compression, were then developed to try to reproduce these conditions as closely as possible. Jaspers showed that the Zerilli-Armstrong model provided a somewhat better fit to the experimental data than did the Johnson-Cook model. The Zerilli-Armstrong model is also better motivated from a metallurgical point of view, because it is based on a model of thermally activated dislocation motion. However, its form is more complicated, and it contains more parameters, which must be estimated from experimental data, than the Johnson-Cook model. As a result, values of the parameters for many materials are not available in the literature, and it is much less widely used than the Johnson-Cook model in FEA simulations of machining processes. The third model was an overstress power law, an option that is available in Abaqus, which assumes that the ratio of the flow stress at nonzero strain rate to the static yield stress of a material is a tabular function of the equivalent plastic strain rate and temperature. This model

is also harder to fit to data than the Johnson-Cook model, and it is therefore also much less widely used in FEA simulations of machining processes. Overall, in the Abaqus simulations, the three constitutive models led to underpriction of the maximum temperatures in the four sets of experiments. The Johnson-Cook model underpredicted the maximum temperature by as much as 350 °C, the Zerilli-Armstrong model by as much as 300 °C, and the Power-Law model by as much as 150 °C (Davies et al., 2003a, Figure 4).

At NIST, a unique SHPB facility has been in operation for several years (Mates et al., 2008). The Pulse-Heated Kolsky Bar Laboratory combines a precision-engineered SHPB, and a controlled DC electrical pulse-heating system. The flow stress can be measured in samples that have been rapidly pre-heated to temperatures on the order of 1000 °C, in a time on the order of one second, at heating rates of up to $6000\,^{\circ}\mathrm{C\,s^{-1}}$, and then rapidly loaded in compression at strain rates up to $10^4\,\mathrm{s^{-1}}$. In recent NIST work on AISI 1045, we have focused our attention on fitting the pulse-heated material response to the Johnson-Cook constitutive model,

$$\sigma_{eq} = [A + B\epsilon^n]\left[1 + C\log\left(\frac{\dot{\epsilon}}{\dot{\epsilon_0}}\right)\right]\left[1 - \left(\frac{T - T_r}{T_M - T_r}\right)^m\right]. \qquad (2.2)$$

In Eq. (2.2), $\dot{\epsilon_0} = 1\,s^{-1}$, and $T_r = 20\,^{\circ}\mathrm{C}$ and $T_M = 1460\,^{\circ}\mathrm{C}$ are room temperature and the melting temperature of the material, respectively.

The five Johnson-Cook parameter values that were determined by Jaspers and Dautzenberg (2002) are given in Table 2. Peak temperatures predicted

A	B	C	n	m
553.1 MPa	600.8 MPa	0.134	0.234	1.0

Table 2: Parameter values for the Johnson-Cook model of Jaspers and Dautzenberg (2002) for AISI 1045 steel.

in FEA simulations of the four tests in Table 1, using this constitutive model for AISI 1045, are plotted in Figure 2 (bottom curve).

In our work, we have demonstrated that AISI 1045 exhibits a stiffer response when it has been pulse-heated prior to testing on a Kolsky bar (Burns et al., 2012), than has been reported by Jaspers and Dautzenberg, who used a slower method for preheating their test samples. Figure 3 gives a plot of the true effective shear stress versus true effective strain data from a pulse-heated Kolsky bar test that was performed at a true strain rate of $3600\,\mathrm{s^{-1}}$. In this test, the sample was heated to a temperature of 643 °C in approximately one second, and then it was held at that temperature

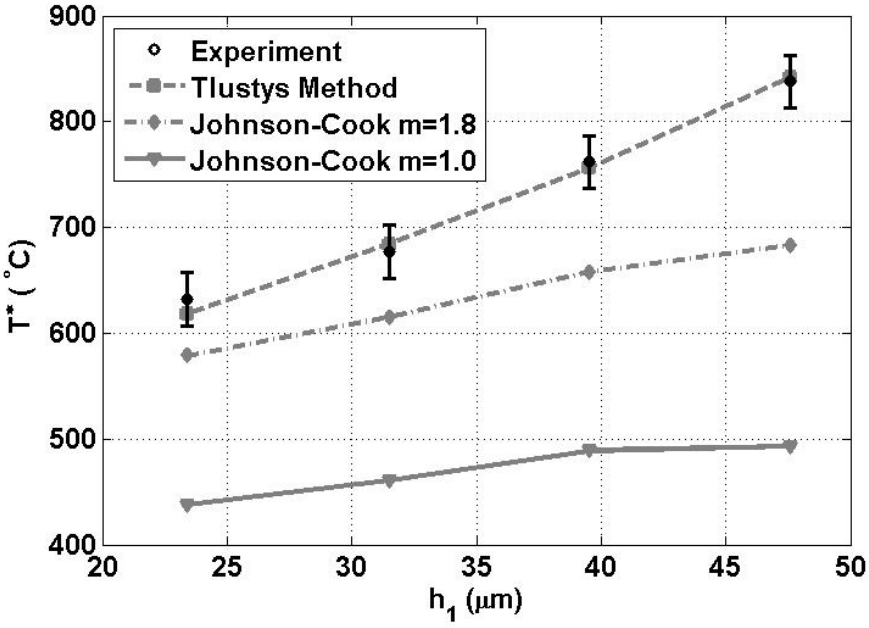

Figure 2: Peak temperature on tool face: experiment vs. simulations. Error bars denote combined standard uncertainty (Davies et al., 2003b).

for approximately 6.2 seconds prior to compressive loading. Also shown in the figure are two additional plots, both using the model of Jaspers and Dautzenberg at the same strain rate and temperature, but with $m = 1.0$ in the lower curve, and $m = 1.8$ in the upper curve. (In Burns et al. (2012), the value $m = 1.7$ was used; here, we use $m = 1.8$, which gives more of an upper bound on the experimental data, and corresponds to slightly less thermal softening. A peculiarity of the Johnson-Cook model is that a *larger* value of the thermal-softening parameter m corresponds to *less* thermal softening.) It is clear that the case with $m = 1.8$ provides a much better fit to the experimental data than does the original model with $m = 1.0$. This is an instance of the fact that irreversible plastic deformation depends upon the deformation substructure in the material, so that the material response is path-dependent, in the sense that its mechanical behavior depends upon the strain path and the temperature and strain rate history (Meyers, 1994; Mates et al., 2009).

The testing conditions that produced the data in Figure 3 are still not nearly as extreme as the conditions in the work material during a typical high-speed orthogonal cutting operation; see e.g., Jaspers (1999). This means, for example, that material response data with a peak strain rate of 3600 s^{-1} and a peak strain of less than 0.3 must be extrapolated to strain rates on the order of $20,000$ s^{-1}, and to strains of 2.0 or greater. Some researchers have asserted that, in the secondary shear zone, the strain-hardening effect should be negligible for $\epsilon > 1$; see Zorev (1966); Oxley (1989); Childs et al. (2000). It would thus follow that the parameter n in (2.2) should be set equal to zero when $\epsilon > 1$. However, this was not done in the simulations using Abaqus/Explicit in the study of Davies et al. (2003a). Had this been done, the underprediction of temperature on the rake face would have been even larger.

We have repeated the Abaqus simulations in Davies et al. (2003a), using the Johnson-Cook model in Jaspers and Dautzenberg (2002) for the four different depths of cut, keeping everything the same, except that this time the thermal-softening parameter was set equal to $m = 1.8$. The peak temperature results are plotted in Figure 2 (center, dot-dashed curve). Compared with the results from the simulations that used $m = 1.0$, the Johnson-Cook model with less thermal softening gives much better peak temperature predictions. Nevertheless, the experimental results are still underpredicted by as much as 150 °C.

It is natural to investigate whether there might be a method for determining the flow stress of the chip material using a machining test. As was discussed in the Introduction, there have been some significant advances in

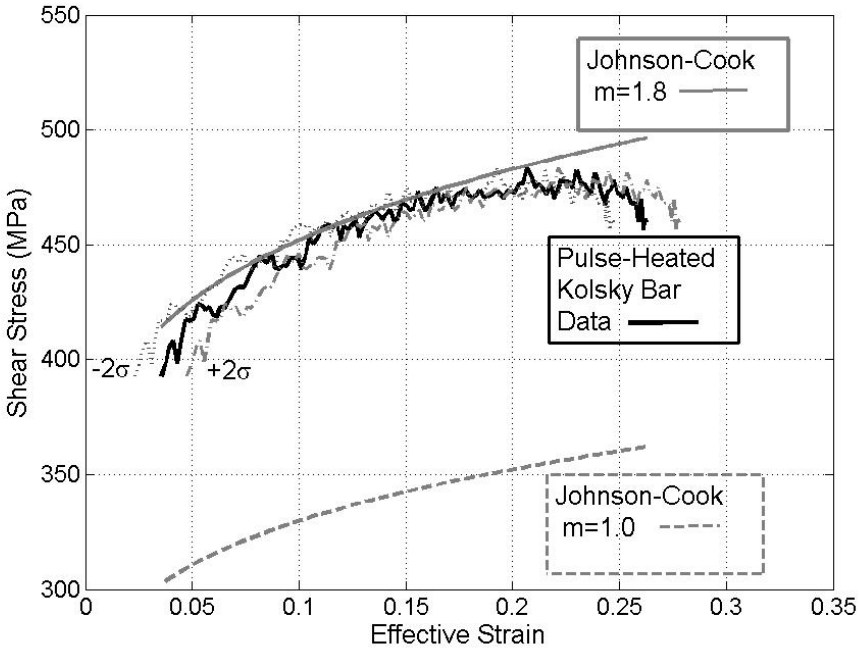

Figure 3: Data from a pulse-heated compression test of an AISI 1045 steel sample that had been preheated to 643 °C, and then plastically deformed, at a true strain rate of 3600 s^{-1}, (solid curve, shown with $\pm 2\sigma$ curves (Burns et al., 2012)). Also shown are Johnson-Cook model curves for AISI 1045, with parameter values in Table 2. In the lower (dashed) curve, $m = 1.0$; in the upper (dot-dashed) curve, $m = 1.8$.

the measurement of temperature on the tool-chip interface during orthogonal cutting tests. Thus, the question arises, is there a way to estimate the shear stress τ in the chip, near the tool-chip interface, given good temperature measurements along this interface? Our approach to this problem has been motivated by analyzing a comparatively simple finite-difference model of Tlusty (2000) for calculating the temperature in the chip. This model was used by Davies et al. (2003b) to produce the top, dashed curve in Figure 2. For reasons that have already been discussed in the Introduction, this method cannot be considered predictive. However, as will be discussed in Section 4, a detailed analysis of this model shows that it can be inverted, so that given an estimate of the temperature T_s of the chip material as it exits the primary shear zone, and an estimate of the peak temperature in this material on the rake face, an estimate can be obtained of τ in the contact region on the rake face. In Section 5, we will show how this approach can be generalized, to obtain a new method for estimating the shear stress in the chip on the rake face. An outline of Tlusty's Method is given in the next section.

3. Tlusty's Method

Tlusty's Method (Tlusty, 2000) estimates the temperature distribution in the chip by making a number of simplifying assumptions. The method starts with the idealized chip flow model in Figure 1, and a model for the transfer of heat in a moving material, the steady-state convection-diffusion equation

$$\rho\, c\, v_f \frac{\partial \tilde{T}}{\partial \tilde{X}} = k \left(\frac{\partial^2 \tilde{T}}{\partial \tilde{X}^2} + \frac{\partial^2 \tilde{T}}{\partial \tilde{Y}^2} \right), \tag{3.1}$$

on the domain

$$0 \le \tilde{X}, \qquad 0 \le \tilde{Y} \le h_2, \tag{3.2}$$

where v_f is the chip velocity, and

$$\tilde{T}(0, \tilde{Y}) = T_s. \tag{3.3}$$

Here, a "tilde" superscript is used to denote a dimensional quantity which will be rendered dimensionless in the next section. The boundary value T_s is the temperature of the work material as it exits the primary shear zone. The method used by Tlusty for calculating T_s is due to Boothroyd (see Boothroyd and Knight (1989)), and it requires several simplifying assumptions. Among these are that the primary shear zone is a planar region of zero thickness and width b, with uniform temperature T_s. In addition, a fixed percentage of heat is assumed to be carried away by the chip, and the remainder is transferred by conduction into the uncut chip material (in Davies et al. (2003b), 80 % was assumed to be convected by the chip).

The generation of heat in the chip by friction near the rake face of the tool is modeled by the boundary condition

$$-k \frac{\partial \tilde{T}}{\partial \tilde{Y}}(\tilde{X}, 0) = \tilde{Q}(\tilde{X}) = \tilde{\tau}(\tilde{X})\, v_f. \tag{3.4}$$

Thus, just as with earlier simplified models, starting with Rapier's, as discussed in the Introduction, Tlusty's model treats heat production on the rake face as a boundary condition; thus, it does not include a flow zone of finite thickness.

In Equation (3.4), $\tilde{\tau}(\tilde{X})$ is the local value of the shear stress on the rake face. The function $\tilde{Q}(\tilde{X})$ is the friction power density; it is nonzero only along the surface of contact between the tool and the chip on the rake face. This surface is also assumed to be planar, and of uniform width b, for $0 \le \tilde{X} \le L_c$. Citing the split-tool results of Buryta et al. (1994), Tlusty

assumed that there is a two-zone contact region, with a sticking region of length L_p near the tooltip, and a sliding region of length $L_e = L_c - L_p$, on the remainder of the tool-chip contact zone, such that the shear stress is given by the piecewise-linear model

$$\tilde{\tau}(\tilde{X}) = \begin{cases} \tau_f & 0 \le \tilde{X} \le L_p \\ \tau_f \left[1 - \left(\tilde{X} - L_p\right)/L_e\right] & L_p \le \tilde{X} \le L_c \\ 0 & L_c \le \tilde{X} \end{cases} \tag{3.5}$$

The friction force on the contact region is then given by

$$F = \int_0^{L_c} \tilde{\tau}(\tilde{X})\, b\, d\tilde{X} = \tau_f\, b \left(L_p + \tfrac{1}{2} L_e\right), \tag{3.6}$$

and the corresponding friction power has the explicit form

$$\Pi_f = F\, v_f = \tau_f\, b \, \left(L_p + \tfrac{1}{2} L_e\right)\, v_f. \tag{3.7}$$

Tlusty also made the simplifying assumptions that

$$L_p = \tfrac{1}{2}\, h_1, \qquad L_c = 4\, h_1. \tag{3.8}$$

In general, these lengths depend upon the cutting speed v_c (Childs et al., 2000; Molinari et al., 2012).

The maximum stress on the rake face τ_f was determined iteratively. Initially, τ_f was set equal to τ_s, the stress on the primary shear plane. There is no theoretical reason for making this assumption; it is simply a way to initialize the code. τ_s was determined using an assumed value of the specific cutting energy K_c, and the uncut chip area $A_c = h_1\, b$. Fixed values for the chip thickness ratio $r = h_1/h_2$ and for the shear plane angle, $\phi = \arctan r$, were also assumed, which is not generally the case.

Following Rapier (1954); Weiner (1955); and Boothroyd (1963), Tlusty assumed that convection is the dominant heat-transport mechanism in the direction of chip flow, so that conduction in the direction $\tilde{X}$ could be neglected. Instead of solving the 2D steady-state equation (3.1), his resulting finite-difference code solves the following transient convection-diffusion problem

$$\rho\, c \left(\frac{\partial \tilde{T}}{\partial \tilde{t}} + v_f\, \frac{\partial \tilde{T}}{\partial \tilde{X}}\right) = k\, \frac{\partial^2 \tilde{T}}{\partial \tilde{Y}^2}, \tag{3.9}$$

on a rectangular grid bounded by

$$0 \le \tilde{X} \le \tfrac{3}{2} L_c, \qquad 0 \le \tilde{Y} \le h_2, \tag{3.10}$$

with uniform initial temperature $\tilde{T} = T_s$, and boundary conditions (3.3) and (3.4). Thus, the left and bottom sides of the grid are bounded by heat sources: the shear plane (3.3), and the plane containing the chip-tool interface (3.4), respectively. The top and right-hand sides of the grid are assumed to be insulated (i.e., convection to the surrounding air is taken to be negligible).

Tlusty's code computes the chip temperature field in two stages. In the first stage, heat transfer from the chip to the tool is neglected, so that all of the friction power generated at the chip-tool interface goes into heating the chip. This part of the code uses a numerical algorithm, which is effectively one-dimensional, that Boothroyd attributed to Dusinberre (1949). During each time step, the code computes the chip temperature in each grid column, a vertical "slice" of material that is insulated on its sides, taking into account heating power inputs from the shear plane and the friction boundary condition on the rake face, but conducting heat only in the direction normal to the rake face. The fixed time increment is the ratio of the grid spacing $\Delta\tilde{X}$ and the cutting speed v_c. After a sufficient number of time steps, the temperature field in the chip reaches a steady-state. This ends the first stage.

In the second stage, the results of the first stage are used to calculate the mean temperature $\bar{T}$ along the tool-chip contact region. The code then determines Π_t, the steady-state rate of heat transfer into the tool. In Tlusty's text, the tool is modeled in discrete form as a two-layer trapezoidal prism of length L_t, uniform width b, and variable cross-sectional area

$$A_t = b\,(L_c + 2\,\tilde{Z}), \qquad 0 \le \tilde{Z} \le L_t, \tag{3.11}$$

with a flat upper layer made of sintered carbide that contacts the chip on the rake face at $\tilde{Z} = 0$, and a second lower layer made of steel. The surface in contact with the chip is assumed to have the mean temperature $\bar{T}$, and the opposite flat surface is assumed to be at room temperature T_r. Using a discrete version of Fourier's Law, Tlusty's algorithm calculates

$$\Pi_t = \left(\bar{T} - T_r\right)/R_t, \tag{3.12}$$

where R_t is an approximation to the thermal resistance of the tool; see, e.g., Incropera and Dewitt (1981) and Appendix A.

The algorithm then adjusts the friction power that goes into heating the chip, by taking into account the rate of heat transfer into the tool. This is done by replacing Π_f by $\hat{\Pi}_f$, where

$$\hat{\Pi}_f = \Pi_f - \Pi_t. \tag{3.13}$$

One way to interpret what this part of the algorithm does is that it adjusts the magnitude of the friction stress from τ_f to $\hat{\tau}_f$, so that (see Eq. (3.7))

$$\begin{aligned} \hat{\Pi}_f &= \tau_f \, b \left(L_p + \tfrac{1}{2} L_e \right) v_f - \left(\bar{T} - T_r \right) / R_t \\ &= \hat{\tau}_f \, b \left(L_p + \tfrac{1}{2} L_e \right) v_f. \end{aligned} \tag{3.14}$$

The procedure is then repeated. The adjusted friction stress magnitude $\hat{\tau}_f$ is used to determine the magnitude of $\tilde{Q}(\tilde{X})$ in the boundary condition (3.4), a new $\bar{T}$ is computed using the first part of the algorithm, then Π_f is readjusted by taking into account the flow of heat into the tool, and so on. The code converges after a few iterations, once the relative error between two successive approximations to $\bar{T}$ is sufficiently small. A description of the finite-difference calculations, including a listing of the code, may be found in Tlusty (2000). Tlusty's Method was used in this way to obtain the estimates for the steady-state temperature fields in Davies et al. (2003b), which by abuse of notation we will denote by $\tilde{T}(\tilde{X}, \tilde{Y})$. The resulting peak temperatures on the rake face are plotted in the top, dashed curve in Figure 2. It is clear that these results could be very different, if different values were assumed for contact length, sticking length, chip thickness ratio, or the thermal resistance of the tool.

In the next section, we will use singular perturbation theory to find an approximation to $\tilde{T}(\tilde{X}, 0)$ that is motivated by Tlusty's Method, and then we will show that the resulting expression can be inverted, so that, given the shear plane temperature T_s and an experimental measurement of the peak temperature T^* along the tool-chip interface, an approximation for the friction stress τ_f can be obtained.

4. Asymptotic Analysis

4.1. Tlusty's Method Revisited

We turn our attention again to the problem defined by Eq. (3.1)-(3.4) in the previous section. First, we scale and nondimensionalize the problem, as follows. Let

$$\Theta = \left(\tilde{T} - T_s\right)/T_s; \quad X = \tilde{X}/L_c; \quad Y = \tilde{Y}/L_c; \quad Q = \tilde{Q}/(\tau_f\, v_f); \quad (4.1)$$

$$X_p = L_p/L_c; \quad X_e = L_e/L_c. \quad (4.2)$$

Then the problem is given in dimensionless form by

$$\frac{\partial \Theta}{\partial X} = \eta \left(\frac{\partial^2 \Theta}{\partial X^2} + \frac{\partial^2 \Theta}{\partial Y^2} \right), \quad (4.3)$$

with boundary conditions

$$\Theta\,(0, Y) = 0, \quad (4.4)$$

and

$$-\delta\, \frac{\partial \Theta}{\partial Y}\,(X, 0) = Q(X), \quad (4.5)$$

where

$$Q(X) = \begin{cases} 1 & 0 \le X \le X_p \\ [1 - (X - X_p)/X_e] & X_p \le X \le 1 \\ 0 & 1 \le X. \end{cases} \quad (4.6)$$

Here,

$$\eta = Pe^{-1}, \quad (4.7)$$

where

$$Pe = (\rho\, c\, v_f\, L_c)/k \quad (4.8)$$

is the Péclet number (Incropera and Dewitt, 1981), and

$$\delta = (k\, T_s)/(L_c\, \tau_f\, v_f). \quad (4.9)$$

In the applications of Tlusty's Method in Davies et al. (2003b), the tool was assumed to consist only of the carbide layer, with length $L_t = 40\,\text{mm}$, and thermal conductivity $k_t = 55.1\,\text{N/s}\cdot^\circ\text{C}$; see Appendix A. Experimental parameters (determined from orthogonal cutting tests in the same workpiece material) included the specific cutting energy and friction angle; these are

K_c (MPa)	λ (deg)	k (N/s · °C)	c (J/kg · °C)	ρ (kg/m^3)
2570	30	43	474	7800

Table 3: Parameter values used for the finite-difference calculations in Davies et al. (2003b) using Tlusty's Method.

Case	h_1 (μm)	T_s (°C)
1	48	479
2	40	487
3	31	496
4	23	502

Table 4: Estimated shear plane temperatures T_s for the four sets of orthogonal cutting experiments in Davies et al. (2003b), using Boothroyd's method. h_1 is the uncut chip thickness.

listed in Table 3. Additional physical parameters for the AISI 1045 that were required for the numerical simulation are also specifed in Table 3. The estimated values of T_s are listed in Table 4.

The parameters η and δ have been defined in Eq. (4.8)-(4.9). Using the estimates $\rho\, c \approx 4\,\mathrm{N/mm^2 \cdot °C}$, $v_f \approx v_c \approx 4\,\mathrm{m/s}$, $h_1 \approx 50\,\mu\mathrm{m}$, so that $L_c = 4\, h_1 \approx 0.2\,\mathrm{mm}$, and $k \approx 50\,\mathrm{N/s \cdot °C}$, we have $\eta \approx \frac{1}{64} \ll 1$. To estimate δ, we use the following additional parameter estimates: $T_s \approx 500\,°\mathrm{C}$ (see Table 4), and $\tau_f \approx 300\,\mathrm{MPa}$. This gives $\delta \approx \frac{5}{48} \ll 1$. We note that both η and δ decrease with increasing cutting speed, and they also decrease with decreasing thermal conductivity. We will take advantage of the smallness of these two parameters by using singular perturbation theory to analyze Tlusty's Method.

In the limit $\eta \to 0$, we get the first-order "outer" equation (see, e.g., Van Dyke (1975))

$$\frac{\partial \Theta}{\partial X} = 0, \tag{4.10}$$

which cannot satisfy both of the specified boundary conditions. The constant function

$$\Theta(X, Y) = 0 \tag{4.11}$$

satisfies the "outer" equation (4.10) and the boundary condition on the primary shear plane at $X = 0$, Eq. (4.4). Thus, to leading order in η, the steady-state chip has the temperature of the shear plane. In order to take into account the significant generation of heat by friction along the tool-chip

interface, which is modeled by the boundary condition (4.5), we introduce the boundary layer coordinate

$$\xi = Y/\sqrt{\eta}, \tag{4.12}$$

which transforms Eq. (4.3) into the "inner" differential equation

$$\frac{\partial \Theta}{\partial X} = \frac{\partial^2 \Theta}{\partial \xi^2} + \eta \, \frac{\partial^2 \Theta}{\partial X^2}, \tag{4.13}$$

and the boundary condition (4.5) into

$$-\frac{\delta}{\sqrt{\eta}} \frac{\partial \Theta}{\partial \xi} \, (X, 0) = Q(X). \tag{4.14}$$

The distinguished limiting case (see, e.g., Van Dyke (1975)) is determined by introducing the similarity parameter

$$\nu = \frac{\sqrt{\eta}}{\delta} = \frac{\tau_f}{T_s} \sqrt{\frac{L_c \, v_f}{\rho \, c \, k}}, \tag{4.15}$$

which we assume remains fixed as $\eta \to 0$ and $\delta \to 0$. Thus, in the boundary layer near the secondary shear zone, we get the leading order problem

$$\frac{\partial \Theta}{\partial X} = \frac{\partial^2 \Theta}{\partial \xi^2}, \tag{4.16}$$

with the boundary condition

$$\frac{\partial \Theta}{\partial \xi}(X, 0) = -\nu \, Q(X). \tag{4.17}$$

We note that Eq. (4.16) is the heat equation, where X is a time-like variable. We require that

$$\Theta(0, \xi) = 0, \text{ and } \Theta(X, \xi) \to 0 \text{ as } \xi \to \infty, \tag{4.18}$$

so that the inner solution approaches the outer solution, Eq. (4.11), away from the boundary layer. The solution to the problem defined by (4.16)-(4.18), which can be obtained by means of the Laplace transform, is given by

$$\Theta(X, \xi) = \frac{\nu}{\sqrt{\pi}} \int_0^X Q(U) \frac{e^{-\xi^2/[4(X-U)]}}{\sqrt{X - U}} dU. \tag{4.19}$$

When $\xi = 0$, we have that

$$\Theta(X,0) \;=\; \frac{\nu}{\sqrt{\pi}}\left\{2\sqrt{X} + \tfrac{4}{3}\left[-H(X-X_p)\,(X-X_p)^{\frac{3}{2}} + H(X-1)\,(X-1)^{\frac{3}{2}}\right]/X_e\right\}; \tag{4.20}$$

here, $H(\cdot)$ is the Heaviside unit step function. The maximum temperature on the rake face occurs when

$$X = X^* = \tfrac{1}{2}\,X_p\,\left[1 + \sqrt{1 + (X_e/X_p)^2}\right], \tag{4.21}$$

and the maximum temperature Θ^* is given by

$$\Theta^* = \nu\,\chi^*, \tag{4.22}$$

where

$$\chi^* = \frac{1}{\sqrt{\pi}}\,\left[2\sqrt{X^*} - \tfrac{4}{3}\,(X^* - X_p)^{\frac{3}{2}}/X_e\right]. \tag{4.23}$$

The mean temperature $\bar{\Theta}$ along the contact region between the tool cutting face and the chip is given by

$$\bar{\Theta} = \int_0^1 \Theta(X,0)\,dX = \nu\,\bar{\chi}, \tag{4.24}$$

where

$$\bar{\chi} = \frac{1}{\sqrt{\pi}}\,\left[\tfrac{4}{3} - \tfrac{8}{15}\,(X_e)^{\frac{5}{2}}\right]. \tag{4.25}$$

Thus, taking into account the rate of heat transfer into the tool, we have that the maximum and mean temperatures along the tool face in the steady state are given, respectively, by

$$T^* = (1 + \hat{\nu}\,\chi^*)\;T_s \qquad \text{and} \qquad \bar{T} = (1 + \hat{\nu}\,\bar{\chi})\;T_s, \tag{4.26}$$

where $\hat{\nu}$ is the modified similarity parameter (see Eq. (4.15)),

$$\hat{\nu} = \frac{\hat{\tau}_f}{T_s}\sqrt{\frac{L_c\,v_f}{\rho\,c\,k}}. \tag{4.27}$$

Just as in Section 3, with Π_t defined by (3.12), $\hat{\tau}_f$ is determined by the "adjusted" friction power (Eq. (3.14)),

$$\begin{aligned}\hat{\Pi}_f \;=\; \Pi_f - \Pi_t \;&=\; \tau_f\,b\left(L_p + \tfrac{1}{2}L_e\right)v_f - \frac{\bar{T} - T_r}{R_t} \\ &=\; \hat{\tau}_f\,b\left(L_p + \tfrac{1}{2}L_e\right)v_f,\end{aligned} \tag{4.28}$$

so that, in the steady state, using Eq. (4.26),

$$\hat{\tau}_f = \tau_f - \frac{[(1+\hat{\nu}\,\bar{\chi})\,T_s - T_r]}{b\,\left(L_p + \frac{1}{2}L_e\right)\,v_f\,R_t}. \tag{4.29}$$

4.2. Inverse Method

Now, instead of using Tlusty's Method to predict the peak temperature in the chip along the face of the tool, assume that we have a measurement of the peak temperature T^* along the tool-work interface, and an estimate T_s of the temperature of the chip material near the tooltip as it exits the primary shear zone. The method that we propose is to use these data and Eqs. (4.26) and (4.27) to obtain an estimate of the shear flow stress during the cutting process. For the piecewise linear two-zone contact model discussed above, using Eq. (4.26), we get the following approximation for the shear stress that corresponds to the modified friction power on the tool rake face, $\hat{\Pi}_f$ (Eq. (4.28)),

$$\hat{\tau}_f = \frac{1}{\chi^*}\sqrt{\frac{\rho\,c\,k}{L_c\,v_f}}\,(T^* - T_s)\,. \tag{4.30}$$

By (4.26),

$$\bar{T} - T_s = (T^* - T_s)\,\bar{\chi}/\chi^*. \tag{4.31}$$

Thus, by (4.29), (4.30) and (4.31), it follows that the shear stress on the tool rake face is given by

$$\begin{aligned}\tau_f &= \hat{\tau}_f + \frac{\bar{T} - T_r}{b\,\left(L_p + \frac{1}{2}L_e\right)\,v_f\,R_t} \\ &= \frac{1}{\chi^*}\sqrt{\frac{\rho\,c\,k}{L_c\,v_f}}\,(T^* - T_s) + \frac{(T^* - T_s)\bar{\chi}/\chi^* + (T_s - T_r)}{b\,\left(L_p + \frac{1}{2}L_e\right)\,v_f\,R_t}.\end{aligned} \tag{4.32}$$

Limitations of this inverse method are that it assumes a specific two-zone model for the shear stress on the rake face, and it requires good estimates of the tool-chip contact length L_c, the length of the sticking region L_p, the shear plane temperature T_s, and the thermal resistance of the tool R_t. In the next section, a generalized inverse method will be presented, that only requires an estimate of R_t.

5. Generalized Inverse Method

5.1. Pure Inverse Problem

Up until now, we have been working with the assumption that a two-zone model has been specified for the friction power distribution on the rake face. In this section, we will address the following question. Suppose that, instead of a contact model, we have been given an experimentally determined discrete set of steady-state temperature measurements along the rake face of the tool, $\{\tilde{T}_i : i = 0, 1, \ldots, N\}$, corresponding, respectively, to the locations $\{\tilde{X}_i : i = 0, 1, \ldots, N\}$ along the rake face, where $\tilde{X}_0$ corresponds to the location closest to the tool tip, $\tilde{X}_i$ for increasing i corresponds to increasing distance from $\tilde{X}_0$, and assume that the work material remains in contact with the tool up to $\tilde{X}_N$. Can we work directly with the experimental data, and obtain an estimate of $\tilde{\tau}(\tilde{X})$, the distribution of the shear stress in the chip along the rake face, without assuming a specific model for the friction along the tool-chip interface? We will next show how the inverse problem of the preceding section can be generalized, so that the answer to this question is "yes."

Let $L_r = \tilde{X}_N - \tilde{X}_0$. Estimates of the peak and mean temperatures in the chip along the contact surface in this case are given by $T^* = \max\{\tilde{T}_i : i = 0, 1, \ldots, N\}$ and $\bar{T} = (1 + N)^{-1} \sum_{i=0}^{N} \tilde{T}_i$, respectively. With the reasonable assumption that the peak temperature is located some distance up the rake face, i.e., $T^* > \tilde{T}_0$, we nondimensionalize and scale the data as follows,

$$X_i = (\tilde{X}_i - \tilde{X}_0)/L_r, \quad \Theta_i = (\tilde{T}_i - \tilde{T}_0)/(T^* - \tilde{T}_0), \quad i = 0, 1, \ldots, N. \quad (5.1)$$

We also assume that we have a sufficiently smooth approximation $\Phi(X)$ to the dimensionless temperature on [0, 1], with $\Phi(0) = 0$. Nondimensionalize $\tilde{\tau}$ as before, $\tau = \tilde{\tau}/\tau_f$, and nondimensionalize $\tilde{Q}$ as in (4.1), so that $Q(X) = \tilde{Q}(\tilde{X}_0 + L_r\, X)/(\tau_f\, v_f)$. By the analysis in Section 4, the temperature and the shear stress are connected by (see (4.19))

$$\Phi(X) = \frac{\hat{\nu}^*}{\sqrt{\pi}} \int_0^X \frac{Q(U)}{\sqrt{X - U}} dU, \quad (5.2)$$

where $\Phi(X) = \Theta(X, 0)$, and

$$\hat{\nu}^* = \frac{\hat{\tau}_f}{T^* - \tilde{T}_0} \sqrt{\frac{L_r\, v_f}{\rho\, c\, k}}. \quad (5.3)$$

Just as in Section 4, the "hat" refers to the "apparent" friction power along the rake face, $\hat{\tilde{Q}}$, which will be adjusted by adding the power absorbed by the tool.

Viewed as an inverse problem, Eq. (5.2) is a Volterra integral equation of the first kind, Abel's equation, for the determination of $Q(X)$ on [0, 1], given $\Phi(X)$. Under mild regularity assumptions on the function $\Phi(X)$, the solution to Eq. (5.2) is well-known (see, e.g., Wing (1991)),

$$\begin{aligned} \frac{\hat{\nu}^*}{\sqrt{\pi}} Q(X) &= \frac{1}{\pi} \frac{d}{dX} \int_0^X \frac{\Phi(U)}{\sqrt{X-U}} dU \qquad (5.4) \\ &= \frac{1}{\pi} \int_0^X \frac{\Phi'(U)}{\sqrt{X-U}} dU. \qquad (5.5) \end{aligned}$$

Let

$$S(X) = \hat{\nu}^* \, Q(X) = \frac{1}{\sqrt{\pi}} \int_0^X \frac{\Phi'(U)}{\sqrt{X-U}} \, dU. \qquad (5.6)$$

Using Eq. (4.1) and (5.3), we get that

$$\begin{aligned} \hat{\tilde{Q}}(\tilde{X}) &= \hat{\tau}_f \, \tau \left((\tilde{X} - \tilde{X}_0)/L_r \right) \, v_f \\ &= \left(T^* - \tilde{T}_0 \right) \sqrt{\frac{\rho \, c \, k \, v_f}{L_r}} \, S \left((\tilde{X} - \tilde{X}_0)/L_r \right). \qquad (5.7) \end{aligned}$$

In this case, the analogue of Eq. (3.14) is given by

$$\begin{aligned} \hat{\Pi}_f &= \tau_f \, b \, v_f \int_{X_0}^{X_N} S \left((\tilde{X} - \tilde{X}_0)/L_r \right) d\tilde{X} - \frac{\bar{T} - T_r}{R_t} \\ &= \hat{\tau}_f \, b \, v_f \int_{X_0}^{X_N} S \left((\tilde{X} - \tilde{X}_0)/L_r \right) d\tilde{X}, \qquad (5.8) \end{aligned}$$

and the analogue of Eq. (4.32) is given by

$$\begin{aligned} \tau_f &= \hat{\tau}_f + \frac{\bar{T} - T_r}{R_t \, b \, v_f \, L_r \int_0^1 S(X) \, dX} \\ &= \left(T^* - \tilde{T}_0 \right) \sqrt{\frac{\rho \, c \, k}{L_r \, v_f}} + \frac{\bar{T} - T_r}{R_t \, b \, v_f \, L_r \int_0^1 S(X) \, dX}. \qquad (5.9) \end{aligned}$$

Thus, given a set of experimentally determined temperature data, the problem of estimating the friction stress along the rake face reduces to solving the integral equation (5.2), and estimating R_t.

5.2. Application of Inverse Method

Unfortunately for our purposes here, the 1D temperature distribution in Ti-6Al-4V along the rake face of the tool in Menon and Madhavan (2015) was determined under cutting conditions in which the chips became shear localized, so that the data are not directly suitable for estimating the shear stress on the rake face. Therefore, we will demonstrate our method using the temperature data from orthogonal cutting tests on AISI 1045 steel in Davies et al. (2003b), that have been described in Section 2 (see Table 1). For this set of four tests, the cutting speed was held constant at 3.7 m/s, while the chip thickness was varied. For each test, ten independent measurements of the 2D temperature field were made, and the mean at each pixel was calculated. The overall uncertainty in these data has been estimated to be $\pm 52\,^{\circ}\mathrm{C}$ at a temperature of $800\,^{\circ}\mathrm{C}$ (Davies et al., 2003b); the errors (in $^{\circ}\mathrm{C}$) have been estimated to be smaller at lower temperatures. From these averaged data sets, 1D temperature traces along the rake face of the tool were determined. There were only 55 data points in each 1D set, and the data were noisy. In the case of the smallest depth of cut, Davies et al. (2003b) noted that the thermal image indicated that the chip may have been curling away from the rake face. For this reason, we have excluded the data set for the smallest depth of cut from our analysis. The 1D data are represented by the solid black curves in Figure 4.

As Wing (1991) points out, when the data are known inexactly at a finite number of points, the numerical inversion of (5.2), based on either (5.4) or (5.5), is unstable. Nevertheless, there are a number of techniques that have been developed for finding an approximate solution of this improperly posed problem; see, e.g., Anderssen and de Hoog (1990); Linz (1985). Here, we have used what appears to be the simplest and most direct method, the product midpoint method. On each subinterval $[X_i,\, X_{i+1}]$ of width ΔX, approximate $S(X)$ by a constant function, $s_{i+\frac{1}{2}}$; approximate the integral on the right-hand side of Eq. (5.2) as a sum of integrals over the subintervals; evaluate each term in the sum using the product rule. This produces the lower-triangular system of equations, for $i = 1, 2, \ldots, N$,

$$\phi_i = \Phi(X_i) = \Sigma_{j=0}^{i-1}\; s_{i+\frac{1}{2}}\, W_{i-j}, \tag{5.10}$$

where

$$W_l = \frac{1}{\sqrt{\pi}} \int_{(l-1)\Delta X}^{l\Delta X} \frac{1}{\sqrt{U}}\; dU = 2\sqrt{\frac{\Delta X}{\pi}}\left(\sqrt{l} - \sqrt{l-1}\right),\; l = 1, 2, \ldots, N. \tag{5.11}$$

Finally, solve the resulting linear system for $s_{i+\frac{1}{2}}$. Under suitable assumptions on the behavior of $\Phi(X)$, this method has been shown to be $O\left(\sqrt{\Delta X}\right)$; see, e.g., Weiss and Anderssen (1972).

Linz (1985) has shown that, asymptotically, a perturbation in ϕ_i of order ε causes a change in the computed solution $s_{i+\frac{1}{2}}$ of order

$$\varepsilon/\sqrt{\Delta X}, \tag{5.12}$$

so that, unless (5.12) is small, the method will amplify noise in the data. Linz states that a satisfactory procedure in this situation is to use some method to smooth the data prior to using the product midpoint method. We have found that an acceptable smoothing for the temperature data in Figure 4 is to filter each data set by averaging the values of successive pairs of points; the smoothed data are represented by the gray dotted curves in the figure.

The thermal resistance of the tool was computed by the method in Appendix A. Using the same assumptions that were used for the simplified tool model in Davies et al. (2003b) (see Section 4), we get that $R_t = 32\,^{\circ}\mathrm{C}\,/\,\mathrm{W}$. Because the $s_{i+\frac{1}{2}}$ are located at the subinterval midpoints, we approximated the integral of S in (5.9) using the midpoint method,

$$\int_0^1 S(X)\,dX \;\approx\; \left(\Sigma_{i=0}^{N-1}\, s_{i+\frac{1}{2}}\right)\Delta X. \tag{5.13}$$

Plots of the resulting shear stress in the work material on the face of the tool, before it was adjusted upward by taking into account the friction power that flows into the tool,

$$\hat{\tilde{\tau}}_f(\tilde{X}) = \left(T^* - \tilde{T}_0\right)\sqrt{\frac{\rho\,c\,k}{L_r\,v_f}}\,S\left((\tilde{X} - \tilde{X}_0)/L_r\right), \tag{5.14}$$

are given in Figure 5. The percentage of frictional energy flowing into the tool was found to be 39, 45, and 56, for $h_1 = 48\,\mu$m, $40\,\mu$m, and $31\,\mu$m, respectively, and the corresponding adjusted final stress estimates are given in Figure 6. The 300 MPa to 350 MPa peak stress values occur some distance up the tool face, in the same order that the peak temperatures occur, but in each case the stress reaches a maximum at a location lower on the tool face than the location where the corresponding peak temperature occurs. The fact that the largest adjusted shear stress peak amplitude in Figure 6 occurs for the smallest depth of cut may not be significant, because the crude model

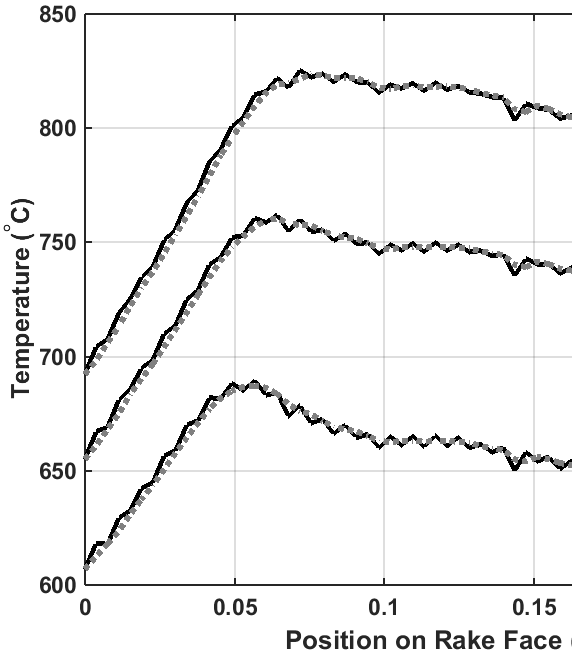

Figure 4: Solid black curves correspond to temperature data from Davies et al. (2003b), for three different depths of cut. The overall uncertainty in these data has been estimated to be $\pm 52\,^{\circ}\mathrm{C}$ at a temperature of $800\,^{\circ}\mathrm{C}$ (Davies et al., 2003b). Dotted grey curves were obtained by averaging the values of successive pairs of points in each data set.

that has been used here for Π_t depends only on the mean temperature along the contact region and the estimated thermal resistance of the tool.

The experiments in Davies et al. (2003b) were performed to measure the temperature in orthogonal cutting, and not to study friction on the tool-chip interface. Whether or not there were zones of sticking on the tool face during the experiments was not determined. It is interesting to speculate, however, on the meaning of the peaks in shear stress in Figures 5 and 6. Based on the study Molinari et al. (2012), it follows from Zorev's constitutive law for the interface (2.1), that if there is a sticking zone on the rake face, then $\tau = \sigma_{eq}/\sqrt{3}$, both on the rake face and in the flow zone. The stress peaks in this case are likely due to strong dependence of the flow stress on temperature. On the other hand, if there is only sliding on the interface, then $\tau = \mu\sigma$; in this case, the form of the shear stress would be consistent with a friction law that depends on the local temperature; see Moufki et al. (1998); Molinari et al. (2011).

Menon and Madhavan (2015) have pointed out that, in the experiments of Davies et al. (2003b), only the side faces of the tool-material interface were visible, and thus only 2D temperature distributions along the intersection of the side planes of the workpiece with the tool have been obtained in these experiments. They argue that the temperatures measured along the side faces, where the material deforms in plane stress, are significantly lower than the temperatures along inner planes, where the material deforms under conditions of plane strain. Also, Wright et al. (1980) have argued that, when sticking occurs, the assumption that the heat source is confined to the interface on the rake face, rather than distributed within the thin flow zone in the chip, may lead to overestimation of the temperatures in the chip and the tool. If these arguments are correct, then this will affect the stress distributions that are given in Figure 5, in a manner that will depend upon the gradients of the estimated 1D temperatures, with respect to increasing distance from the tool tip along the rake face, since the temperature and the shear stress on the rake face are connected by (5.6).

The method of Menon and Madhavan (2015) derives a 1D temperature distribution by aligning their processed thermal image of the rake face vertically, extracting the interior region that includes the centerline, where the gradient of the intensity in the direction of the cutting edge is small, and then averaging the temperature values along vertical columns of pixels to get an average intensity as a function of distance along the rake face. Thus, their method is much less sensitive to the steep temperature gradients that are present in the side view thermal images of Davies et al. (2003b). It will be interesting to compare the results obtained in Figures 4-6 with results

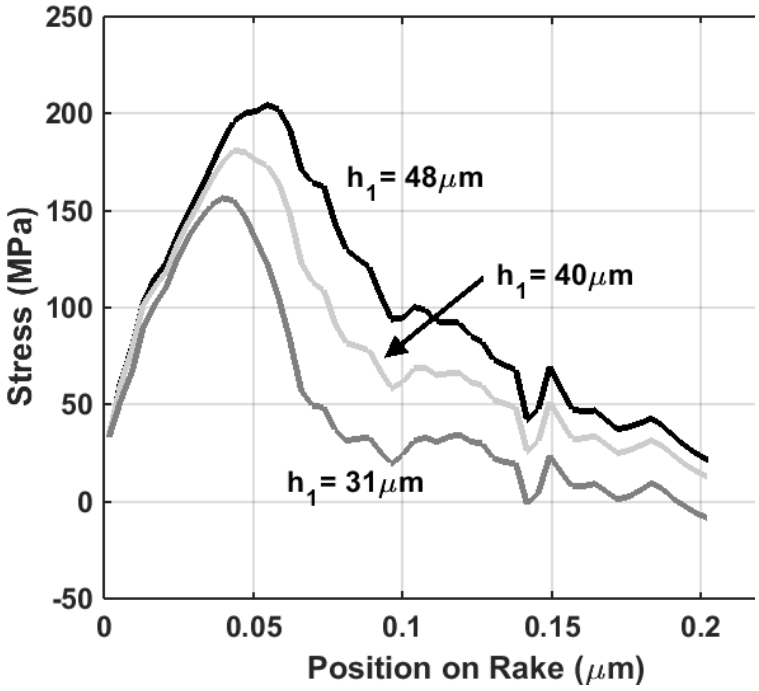

Figure 5: Shear stress (5.14) in the AISI 1045 on the rake face, without correction for heat flow into the tool.

obtained from measurements performed using the YAG tool experimental setup, when they become available.

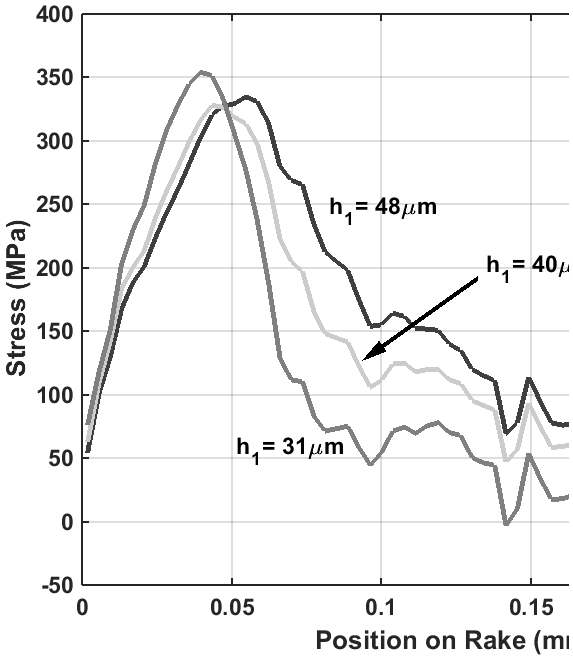

Figure 6: Shear stress in the work material on the rake face, after adjusting $\hat{\tilde{\tau}}_f(\tilde{X})$ upwards by taking into account steady-state friction power absorbed by the tool.

6. Discussion and Concluding Remarks

We have shown that estimates of the shear stress in AISI 1045 steel near the tool rake face during high-speed machining tests, using data from both traditional and pulse-heated split-Hopkinson pressure bar experiments, have produced finite-element simulation results that significantly underpredict peak temperatures that have been measured in orthogonal cutting experiments using non-contact thermometry. A major reason for this lack of agreement between simulation and experiment is almost certainly due to the fact that compression test experimental methods to date cannot reproduce the extreme conditions that are present in the work material during a machining operation. Thus, constitutive laws based on these experimental results give inaccurate predictions of material response during a machining simulation.

The theoretical work in the present paper has been motivated by the recent development by Menon and Madhavan (2015) of an improved design of transparent cutting tools, that are made from cubes of the optical material YAG. These tools enable in-situ observation of the chip-tool interface during orthogonal machining tests, in a cutting system that simultaneously measures the cutting and thrust forces. We have demonstrated that, given a set of steady-state temperature measurements on the rake face, estimation of the corresponding shear stress in the work material near the rake face can be interpreted as an inverse problem. In the case where we have assumed Tlusty's piecewise-linear friction model on the tool-material interface, we have shown that the inverse problem can be solved analytically, given values for the shear plane temperature T_s and the peak rake face temperature T^*. The same kind of approach could be used to treat the inverse problem for the related nonlinear contact friction models of Ozlu et al. (2009, 2010). Our main interest, however, has been to develop a method that can be used to estimate the shear stress, without specifying a friction model. We have shown that, given a set of experimental temperature measurements in the chip along the rake face, the inverse problem of determining the shear stress can be interpreted as a problem requiring the deconvolution and unfolding of an Abel equation, Eq. (5.2), a (weakly) singular Volterra integral equation of the first kind.

With this information, the friction power Π_f consumed by the cutting system can be estimated using Eq. (5.8)-(5.9). Since the method of Menon and Madhavan (2015) enables measurement of the cutting and thrust forces, F_c and F_t, simultaneously with the temperature during orthogonal cutting, the power input Π_m during the cutting test can also be determined. Using

Merchant's Model (Merchant, 1944), the shearing power consumed by the system is given by $\Pi_s = \Pi_m - \Pi_f$. With this estimate, and a measurement of the shear plane angle, one can also estimate the shear stress τ_s in the chip material on the primary shear plane.

No attempt has been made in this paper to use the inverse method to fit a specific constitutive model for the chip material. As pointed out in Section 2, models for the von Mises flow stress of the form

$$\sigma_{eq}(\epsilon, \dot{\epsilon}, T) \tag{6.1}$$

are inadequate, because they lack information about the thermomechanical loading history of a material. Furthermore, whenever there is a sticking region due to friction along the tool face, it follows that $\tau_f = \sigma_{eq}/\sqrt{3} =$ constant, $\dot{\epsilon} = 0$, and $\epsilon =$ constant in the sticking region. However, the analysis in Section 4 (see Eq. (4.6) and (4.20)) shows that, for $0 \leq X \leq X_p$,

$$\Theta(X, 0) = \frac{2\nu}{\sqrt{\pi}} \sqrt{X}. \tag{6.2}$$

Therefore, the temperature is not constant in the sticking region. For a model of the form (2.2), this is not consistent with the condition that $\tau_f =$ constant.

The method for estimating shear stress that has been presented in Section 5 requires a model for the steady-state rate of heat transfer by conduction per unit area into the tool, $\tilde{Q}_t(\tilde{X})$. The simple one-dimensional model for $\tilde{Q}_t$ that is used in Tlusty's Method, as described in Section 3 and Appendix A, assumes that there is a uniform temperature $\bar{T}$ in the chip on the rake face. However, this is not what has been observed experimentally (see, e.g., Boothroyd and Knight (1989); Davies et al. (2003b); Menon and Madhavan (2015)), nor is it what Tlusty's Method predicts (Tlusty, 2000). If there is a sticking region on the rake face, Eq. (6.2) shows that the temperature cannot be uniform in this region. Furthermore, the percentages of frictional energy that flow into the tool, based on use of this model, are very large, $39\,\% - 56\,\%$ (see Section 5), compared to $20\,\%$, which was estimated by Wright et al. (1980). Thus, an open problem for further research is the development of an improved model for the friction power consumed by the tool.

Determination of a model for the flow stress, or even the magnitude of the flow stress, for machining applications, has been a challenging problem for a long time. Given recent progress in the measurement of temperature, together with force, during an orthogonal cutting operation, it is our hope

that the method presented here will contribute to the development of improved machining process models.

Discussions with V. Madhavan, and detailed comments by two reviewers on a preliminary version of this paper, have helped to improve the manuscript, and are gratefully acknowledged.

References

Abaqus (2003). *Abaqus/Explicit Users Manual, Version 6.4*. Hibbit, Karlsson and Sorenson, Inc., Providence, Rhode Island, USA, 2003.

R. S. Anderssen and F. R. de Hoog. Abel integral equations. In Michael A. Golberg, editor, *Numerical Solution of Integral Equations*, chapter 8. Plenum Press, New York, New York, 1990.

D. Basak, H. W. Yoon, R. Rhorer, and T. Burns. Microsecond time-resolved pyrometry during rapid resistive heating of samples in a Kolsky bar apparatus. In *AIP Conference Proceedings*, volume 684, pages 753–757, 2003. doi: 10.1063/1.1627218.

D. Basak, H. W. Yoon, R. Rhorer, T. J. Burns, and T. Matsumoto. Temperature control of pulse heated specimens in a Kolsky bar apparatus using microsecond time-resolved pyrometry. *International Journal of Thermophysics*, 25:561–574, 2004.

G. Boothroyd. Temperatures in orthogonal metal cutting. *Proceedings of the Institution of Mechanical Engineers*, 177(29):789–802, 1963.

G. B. Boothroyd and W. A. Knight. *Fundamentals of Machining and Machine Tools*. Marcel Dekker, New York, New York, USA, second edition, 1989.

T. J. Burns, S. P. Mates, R. L. Rhorer, E. P. Whitenton, and D. Basak. Modelling the peak cutting temperature during high-speed machining of AISI 1045 steel. *Engineering Transactions*, 60:113–124, 2012.

D. Buryta, R. Sowerby, and I. Yellowley. Stress distributions on the rake face during orthogonal machining. *International Journal of Machine Tools and Manufacturing*, 345:721–739, 1994.

T. H. C. Childs, K. Maekawa, T. Obikawa, and Y. Yamane. *Metal Machining: Theory and Applications*. John Wiley and Sons, New York, New York, USA, first edition, 2000.

M. A. Davies, Q. Cao, A. L. Cooke, and R. Ivester. On the measurement and prediction of temperature fields in machining AISI 1045 steel. *CIRP Annals - Manufacturing Technology*, 52:77–80, 2003a.

M. A. Davies, H. Yoon, T. L. Schmitz, T. J. Burns, and M. D. Kennedy. Calibrated thermal microscopy of the tool-chip interface in machining. *Machining Science and Technology*, 7:166–190, 2003b.

D. Dudzinski and A. Molinari. A modelling of cutting for viscoplastic materials. *International Journal of Mechanical Science*, 39:369–389, 1997.

G. M. Dusinberre. *Numerical Analysis of Heat Flow*. McGraw-Hill, New York, New York, USA, 1949.

F. P. Incropera and D. P. Dewitt. *Fundamentals of heat and mass transfer*. John Wiley and Sons, New York, New York, USA, first edition, 1981.

R. W. Ivester, M. Kennedy, M. A. Davies, R. Stevenson, J. Thiele, R. Furness, and S. Athavale. Assessment of machining models: Progress report. *Machining Science and Technology*, 4:511–538, 2000.

S. P. F. C. Jaspers. *Metal Cutting Mechanics and Material Behaviour*. PhD thesis, Technische Universiteit Eindhoven, 1999.

S. P. F. C. Jaspers and J. H. Dautzenberg. Material behaviour in conditions similar to metal cutting: flow stress in the primary shear zone. *Journal of Materials Processing Technology*, 122:322–330, 2002.

G. R. Johnson and W. H. Cook. A constitutive model and data for metals subjected to large strains, high strain rates and high temperatures. In *7th International Symposium on Ballistics*, pages 541–547, The Hague, Netherlands, 1983.

Y. Kakino. Analyses of the mechanism of orthogonal maching by finite element method. *Journal of the Japan Society of Precision Engineering*, 37(7):503–508, 1971.

S. Kalpakjian and S. R. Schmid. *Manufacturing Engineering and Technology*. Prentice-Hall, Upper Saddle River, New Jersey, USA, sixth edition, 2009.

P. Linz. *Analytical and Numerical Methods for Volterra Equations*. SIAM, Philadelphia, Pennsylvania, USA, 1985.

S. P. Mates, R. L. Rhorer, E. P. Whitenton, T. J. Burns, and D. Basak. A pulse-heated Kolsky bar technique for measuring flow stress of metals subjected to high loading and heating rates. *Experimental Mechanics*, 48: 799–807, 2008.

S.P. Mates, S. Banovic, R. Rhorer, T. Burns, E. Whitenton, and D. Basak. An electrical pulse-heated kolsky bar technique for high strain rate flow

stress measurements of rapidly heated metals. In *DYMAT - 9th International Conference on the Mechanical and Physical Behaviour of materials under Dynamic Loading*, volume 1, pages 457–462, Brussels, Belgium, 2009.

T. Menon and V. Madhavan. High accuracy full-field infrared thermography of the chip-tool interface through transparent cutting tools while machining Ti-6Al-4V. In preparation, 2015.

M. E. Merchant. Basic mechanics of the metal cutting process. *ASME Journal of Applied Mechanics*, 11:A168A175, 1944.

M. A. Meyers. *Dynamic Behavior of Materials*. John Wiley and Sons, Inc., New York, New York, USA, 1994.

A. Molinari, R. Cheriguene, and H. Miguelez. Numerical and analytical modeling of orthogonal cutting: The link between local variables and global contact characteristics. *International Journal of Mechanical Sciences*, 53: 183–206, 2011.

A. Molinari, R. Cheriguene, and H. Miguelez. Contact variables and thermal effects at the tool-chip interface in orthogonal cutting. *International Journal of Solids and Structures*, 49:3774–3796, 2012.

A. Moufki, A. Molinari, and D. Dudzinski. Modelling of orthogonal cutting with a temperature dependent friction law. *Journal of the Mechanics and Physics of Solids*, 46(10):2103–2138, 1998.

P. L. B. Oxley. *Mechanics of Machining*. Ellis Horwood, Ltd., West Sussex, England, 1989.

E. Ozlu, E. Budak, and A. Molinari. Analytical and experimental investigation of rake contact and friction behavior in metal cutting. *International Journal of Machine Tools and Manufacture*, 49:865–875, 2009.

E. Ozlu, A. Molinari, and E. Budak. Two-zone analytical contact model applied to orthogonal cutting. *Machining Science and Technology*, 14: 323–343, 2010.

A. C. Rapier. A theoretical investigation of the temperature distribution in the metal cutting process. *British Journal of Applied Physics*, 5:400–405, November 1954.

R. L. Rhorer, M. A. Davies, M. D. Kennedy, B. S. Dutterer, and T. J. Burns. Construction and alignment of a Kolsky bar apparatus. In *ASPE Proceedings*, St. Louis, Missouri, 2002. American Society for Precision Engineering.

M. C. Shaw. *Metal Cutting Principles*. Oxford University Press, New York, New York, USA, 1984.

T. Shirakashi and E. Usui. Simulation analyses of orthogonal metal cutting. *Journal of the Japan Society of Precision Engineering*, 42(5):340–345, 1976.

F. W. Taylor. On the art of cutting metals. *Transactions of the ASME*, 28: 31–350, 1907.

J. Tlusty. *Manufacturing Processes and Equipment*. Prentice-Hall, Upper Saddle River, New Jersey, USA, 2000.

E. M. Trent and P. K. Wright. *Metal Cutting*. Butterworth-Heinemann, Woburn, Massachusetts, USA, fourth edition, 2000.

E. Usui and T. Shirakashi. Mechanics of machining - from descriptive to predictive theory. In *On the art of cutting metals–75 years later : a tribute to F.W. Taylor, ASME Publication PED 7*, pages 13–85, 1982.

M. Van Dyke. *Perturbation Methods in Fluid Mechanics*. The Parabolic Press, Stanford, California, USA, annotated edition, 1975.

J. H. Weiner. Shear-plane temperature distribution in orthogonal cutting. *Transactions of the American Society of Mechanical Engineers*, 77(8): 1331–1341, 1955.

R. Weiss and R. S. Anderssen. A product integration method for a class of singular first kind volterra equations. *Numerische Mathematik*, 18: 442–456, 1972.

E. P. Whitenton. The NIST kolsky bar data processing system. In *SEM Annual Conference and Exposition on Experimental and Applied Mechanics*, Portland, Oregon, USA, 2005.

G. M. Wing. *A Primer on Integral Equations of the First Kind*. SIAM, Philadelphia, Pennsylvania, USA, 1991.

P. K. Wright and E. M. Trent. Metallurgical appraisal of wear mechanism and processes on high speed steel cutting tools. *Metals Technology*, 1: 13–23, 1974.

P. K. Wright, S. P. McCormick, and T. R. Miller. Effect of rake face design on cutting tool temperature distributions. *Journal of Engineering for Industry*, 102:123–128, 1980.

H. W. Yoon, D. Basak, R. L. Rhorer, E. P. Whitenton, T. J. Burns, R. J. Fields, and L. E. Levine. Thermal imaging of metals in a kolsky-bar apparatus. In *Thermosense XXV*, volume 5073, pages 284–294. SPIE, 2003. doi: 10.1117/12.488111.

F. J. Zerilli and R. W. Armstrong. Dislocation mechanics based constitutive relations for material dynamics calculations. *Journal of Applied Physics*, 61:1816–1825, 1987.

O. C. Zienkiewicz. *The Finite Element Method in Engineering Science*. Mc Graw Hill, London, second edition, 1971.

N. N. Zorev. Inter-relationship between shear processes occurring along tool face and shear plane in metal cutting. In *International Research in Production Engineering*, New York, New York, 1963. American Society for Mechanical Engineering.

N. N. Zorev. *Metal Cutting Mechanics*. Pergamon Press, Oxford, United Kingdom, first English edition, 1966.

Appendix A. Simplified Tool Model

Assumptions:

1. Steady-state heat conduction;

2. No internal heat generation;

3. One-dimensional conduction in $\tilde{Z}$ direction (normal to rake face);

4. Surface in contact with the chip has uniform temperature $\bar{T}$; opposite surface is at room temperature T_r;

5. Cross-sectional area of the tool increases linearly in the direction normal to the surface of contact with the chip:

$$A_t = b\,(L_c + 2\,\tilde{Z}); \tag{A.1}$$

6. Constant material properties: heat conductivity of the tool k_t = constant;

7. Rate of heat transfer from the rake face into the tool is governed by Fourier's Law (see, e.g., Incropera and Dewitt (1981)):

$$\Pi_t = -k_t\,A_t \frac{d\tilde{T}}{d\tilde{Z}}. \tag{A.2}$$

By Eq. (A.2), it follows that

$$\Pi_t \int_0^{L_t} \frac{d\tilde{Z}}{A_t(\tilde{Z})} = -k_t \int_{\bar{T}}^{T_r} d\tilde{T}. \tag{A.3}$$

Therefore, the heat transfer rate into the tool is given by Eq. (3.12),

$$\Pi_t = \left(\bar{T} - T_r\right)/R_t,$$

where R_t is the thermal resistance of the tool, which is given by

$$R_t = \frac{\ln\left(1 + 2\,L_t/L_c\right)}{2\,b\,k_t}. \tag{A.4}$$

List of Tables

List of Figures